Journal of Experimental Botany, Vol. 58, No. 3, pp. 717–732, 2007
doi:10.1093/jxb/erl244 Advance Access publication 21 December, 2006
This paper is available online free of all access charges (see http://jxb.oxfordjournals.org/open_access.html for further details)

Journal of Experimental Botany

RESEARCH PAPER

Patterns and kinetics of water uptake by soybean seeds

Chris J. Meyer[1], Ernst Steudle[2] and Carol A. Peterson[1,*]

[1] *Department of Biology, University of Waterloo, Waterloo, ON, Canada N2L 3G1*

[2] *Department of Plant Ecology, University of Bayreuth, D-95440 Bayreuth, Germany*

Received 1 June 2006; Revised 23 October 2006; Accepted 25 October 2006

Abstract

Soybean [*Glycine max* (L.) Merr.] plants produce some seeds (called stone or impermeable seeds) that do not take up water for long periods of time. The present investigation confirmed that the stone seed trait is a feature of the seed coat: isolated embryos from both stone and permeable seeds took up water equally quickly. A whole, permeable seed typically imbibed water initially through its dorsal side, forming wrinkles in the seed coat and delivering water to the underlying cotyledons. Later, some lateral movement of water through the coat occurred, presumably through the air spaces of the osteosclereid layer. Imbibition by seeds was a two-phase process, the first dominated by hydration of the seed coat and the second by hydration of the cotyledons, which was rate-limited by the coat. When hydrated, coats of stone seeds were permeable to water but their hydraulic conductivity, as measured with a pressure probe, was smaller than that of coats from permeable seeds by a factor of five. Hydrated coats of both permeable and stone seeds showed weak osmometer properties.

Key words: Cuticle, *Glycine max*, hydraulic conductivity, imbibition, seed coat.

Introduction

Plants from ~15 families, including legumes (Fabaceae), possess a feature known as hardseededness (Arechavaleta-Medina and Snyder, 1981; Calero *et al*., 1981; Hill *et al*., 1986; Baskin *et al*., 2000). Such plants produce a certain fraction of seeds that imbibe water readily and others that are impervious to water, even after long periods of soaking. Recently, Ma *et al*. (2004) reported that the critical difference between permeable and impermeable (stone) seeds of soybean is the continuity of the outermost cuticle. Small cracks, visible with scanning electron microscopy (SEM), were present in cuticles of permeable seeds but were absent in those of stone seeds so that water was not admitted to any part of the latter seed type. In the former type of seed, the first visible sign of imbibition was wrinkling of the seed coat typically on the dorsal side, the location of the majority of the very small cracks in the cuticle.

It is assumed that the general function of seed coats during imbibition is to allow water entry to the enclosed embryo but to restrict the flow somewhat so that hydration does not proceed too rapidly (Bewley and Black, 1978; McDonald *et al*., 1988). Such rapid water uptake may lead to cell damage that can negatively affect germination and growth (Larson, 1968; Bewley and Black, 1978; Powell and Matthews, 1978; Hahalis *et al*., 1996). Even with an intact seed coat, there may be a time period during the early stages of imbibition in which solutes are lost from the cells of the embryo (Larson, 1968; Parrish and Leopold, 1977; Bewley and Black, 1978; Powell and Matthews, 1978; Duke *et al*., 1983). Therefore, quantifying the permeability of the seed coat to water and solutes would be of great importance.

In the present study, it proved possible to measure directly the permeability of isolated seed coats to water (hydraulic conductivity, *Lp*), under standard conditions, using a pressure probe and an osmometer. With the former instrument, a bulk flow of water through the coat was induced and the hydraulic conductivity (the inverse of the hydraulic resistivity) of the coat measured. Using the osmometer, an instrument used in the past to measure the

* To whom correspondence should be addressed. E-mail: cpeterson@uwaterloo.ca

Abbreviations: β, elastic modulus of pressure probe; ϵ, elastic modulus of osmometer; π^i, osmotic pressure of a cell; π°, osmotic pressure of medium; *A*, surface area; Lp_h, hydrostatic hydraulic conductivity; Lp_o, osmotic hydraulic conductivity; *P*, pressure in probe or osmotic cell; P_s, solute permeability of seed coat; RO, reverse osmosis; SEM, scanning electron microscopy; $T^s_{1/2}$, half-time of solute permeability of seed coat; $T^w_{1/2}$, half-time of water permeability of seed coat.

osmotic properties of reverse osmosis (RO) membranes (Steudle and Heydt, 1988), gradients in osmotic pressure were introduced so osmotic water flows across isolated seed coats could be measured. Additionally, the leakage (permeation) of certain salts and organic solutes was estimated with this device. One would expect that the water flow induced in the presence of a pressure (hydrostatic Lp_h) would be larger than that measured in the presence of an osmotic gradient (osmotic Lp_o; Steudle and Peterson, 1998). This is so because there should be some apoplastic water movement across the barrier. For roots, it has been shown that this causes differences depending on the nature of the driving force (Zimmermann and Steudle, 1998; Ranathunge *et al*., 2003).

Water uptake by seeds from soil follows a gradient in water potential. On the soil side, this potential is usually dominated by matric forces (Kramer and Boyer, 1995). On the dry seed side, the water potential should be influenced by matric and osmotic components (Vertucci, 1989), although the former is likely to be dominant. As seeds hydrate, water flows are controlled by local conductivities and storage capacities for water (i.e. by 'diffusivities') besides the coat, and are driven by gradients of water potential. Hence, information about differences between the Lp_h and Lp_o of seed coats may be valuable.

The present study was designed to answer several questions regarding soybean seed hydration.

1. Does the location of the initial wrinkles in the seed coat correlate with the location of the initial hydration of the underlying cotyledons?
2. After hydration of a specific zone of the seed coat, does it play a special role in facilitating lateral movement of water within itself? Could this help to distribute water evenly in the seed as suggested by McDonald *et al*. (1988)?
3. Is there any uneven hydration of the cotyledons due to differential hydration of the seed coat, or is it partly or entirely due to differences in the hydration capability of the cotyledons?
4. Does the hydration of the seed follow first-order kinetics as described by Leopold (1983)? If so, this may indicate a rate limitation of uptake by the coat rather than by the hydration of the cotyledons. Otherwise one would expect a more complicated pattern of water uptake.
5. How much does the water permeability of hydrated coats of stone seeds differ from that of permeable seeds?

Materials and methods

Plant material

Seeds of soybean [*Glycine max* (L.) Merr.] were obtained from plants grown outdoors at Agriculture and Agri-Food Canada in London, Ontario, in 2003. Mature pods were picked and their seeds carefully removed by hand. Prior to use, seeds were air-dried and stored in the laboratory (~23 °C; 30–50% relative humidity). Seeds from a variety that produces predominantly permeable seeds (cv. Harovinton) were screened with a dissecting microscope; only those without visible physical defects, such as cracks or necroses, were retained. Impermeable seeds from cv. OX 951 were identified by weighing before and after soaking in water for 24 h. Seeds that had not gained weight were considered to be impermeable, and were air-dried and used in subsequent experiments.

Visible aspects of seed hydration

Seeds of cv. Harovinton were hydrated either by submerging them in tap water or by surrounding them with water-saturated filter paper. Externally visible changes such as seed coat wrinkling and increases in seed size were followed during periods of up to 10 h. Seeds were removed at the desired intervals and photographed with a Carl Zeiss, Vario-sonar Cyber-shot 3.3 Megapixel lens assembly attached to a Sony DSC-F505V digital camera. In some cases, seed coats were partially removed to show the desired areas of the underlying cotyledons. Some seeds were then bisected longitudinally and transversely to observe the internal hydration fronts. In a second set of experiments, seed coats were removed prior to soaking. Specimens were illuminated by two incident light sources positioned opposite to each other and adjusted so that wet areas of the cotyledons appeared darker yellow in comparison with dry areas. Seed parts were observed with a dissecting microscope (Carl Zeiss Canada, Don Mills, Ontario, Canada), and photographed with a digital camera (Q-Imaging, Retiga 2000R, Fast 1394, Cooled Mono, 12-bit; Quorum Technologies Inc., Guelph, Ontario, Canada).

To assess the importance of the seed coat in conducting water laterally (circumferentially) during imbibition, water was supplied to seeds on their dorsal, ventral, or abaxial sides. Petroleum jelly was applied at the border of the area to be tested to confine the water to the treatment area. The seed was then placed on a short, plastic ring that had been cut open on one side to allow for seed expansion. This assembly was lowered onto a piece of water-saturated filter paper in a small Petri dish and the dish was covered. After the desired time, the seeds were removed, cut, observed, and photographed with the digital camera described above. Ten seeds were used for each hydration treatment described above.

Intercellular spaces of the osteosclereid layer

To measure the sizes of the intercellular spaces between the column-like parts of the osteosclereids in the seed coats of cv. Harovinton, small portions of the coats were removed from the ventral, abaxial, and dorsal sides of eight seeds. Specimens were briefly hydrated in water, stained with 0.01% (w/v) Cellufluor (Polysciences; Warrington, PA, USA) for 1 min, rinsed with water, cross-sectioned, and viewed with ultraviolet (UV) light using a Zeiss Axiophot epifluorescence microscope (filter set: exciter filter G 365, dichroitic mirror FT 395, and barrier filter LP 420; Carl Zeiss Canada). Photographs of these coats were taken with the digital camera described above, and printed so that the spaces between osteosclereids could be measured manually.

Kinetics of water uptake by whole seeds

For a quantitative analysis of rates of imbibition, 10–12 seeds for each of cvs Harovinton and OX 951 were weighed to an accuracy of 0.1 mg, then submerged in tap water. Seeds were blotted, reweighed, and returned to the water at the desired times (i.e. at 1 min intervals during the initial 2 h and subsequently up to 60 min intervals). Imbibition continued until the seeds attained a constant maximum weight (w_{max}) or nearly so. In a second set of

experiments, the seed coats of both cultivars were removed prior to imbibition.

In the past, the rate of seed swelling during hydration has often been described as being analogous to the imbibition of polymers by solvents (for references, see Leopold 1983). In these kinetics, the rate of solvent uptake (water), dw/dt, was assumed to be linearly related to the water deficit in the seed which is $w_{max}-w$. Here, w_{max} is its weight at full hydration and w is the actual weight of a seed at time t. The linear relationship assumes that the water deficit would also be linearly related to the difference in water potential between the seed and its surroundings, which is the force driving water uptake. The following relationship should be valid:

$$\frac{dw}{dt} = k(w_{max} - w). \quad (1)$$

Provided that the rate constant of water uptake, k, does not change during hydration, Eq. (1) may be integrated to yield an exponential time-course of hydration, as has often been observed in the literature (Leopold, 1983),

$$w = w_{max} \cdot (1 - \exp(-kt)) \text{ or } -kt = \ln\left(\frac{w_{max} - w}{w_{max}}\right). \quad (2)$$

In this model, it is assumed that the seed coat, rather than the seed interior, limits imbibition. Therefore, determining the hydraulic conductivity of the seed coat would be important. However, the latter parameter could only be worked out from k, when the forces driving the movement of water across the coat are known, i.e. the water potential difference, which is difficult to measure.

In an alternative model, also used in seed physiology, one may assume that the coat does not represent a significant resistance so that water moves across a rather homogenous seed, largely made up of the cotyledons. In this case, movement across the seed should follow diffusion kinetics, i.e. movement from one differential shell layer to the next should be driven by differences in water potentials between shells analogous to Fick's first law of diffusion. Then the rate of swelling of a seed would be governed by the so-called 'diffusivity' (D) that has the units of a diffusion coefficient ($m^2\ s^{-1}$), but represents a mass displacement of water rather than a diffusive flow governed by a diffusion coefficient (Philip, 1958; Molz and Ikenberry, 1974; Steudle and Boyer, 1985; Vertucci, 1989; Steudle, 1992). The processes of diffusion and diffusivity are fundamentally different in nature, although they are formally described by the same type of mathematics, which differs from the simple exponential type of kinetics given in Eqs (1) and (2). In fact, in some of the experiments, deviations from the simple exponential behaviour were seen that may be better described by a diffusion type of kinetics. The soybean seeds used in this study may be approximated as spheres with a radius (r) of ~3.5 mm (see Results). It is expected that seed weight (w) will increase as imbibition proceeds, provided that the spherical seeds behave like a homogenous material with a constant diffusivity (D) during swelling, as described by Crank (1975):

$$\frac{w}{w_{max}} = 1 - \frac{6}{\pi^2}\sum_{n=1}^{\infty}\frac{1}{n^2}\exp(-D \cdot n^2\pi^2 t/r^2). \quad (3)$$

It is stated in Eq. (3) that the process can be described by a complicated sum of exponentials that contain certain constants. The terms on the right side of Eq. (3) with high values of n should rapidly decline during the water uptake by a seed. Consequently, there should be a pronounced linear range (when water uptake is plotted logarithmically versus time). This is so because, as the hydrated outer layer grows, its hydraulic resistance increases. At a certain thickness, the hydrated layer may act as some kind of a 'coat' and kinetics then tend to become formally similar to those given in Eq. (2). The difference between the exponential and diffusion kinetics is that the latter are usually faster than exponential at early stages before they tend to become exponential.

In the current work, it was expected to see a diffusion type of kinetics with decoated seeds and an exponential type with the coated seeds. Things may be complicated by the fact that during hydration, the constants k and D may vary, namely during the early stages of imbibition. Also, diffusivities may be different in seed coats as compared with the inner parts of seeds due to anatomical differences.

Hydraulic conductivity of isolated seed coats

Seed coat preparation: A piece of seed coat ~8 mm in diameter, still connected to parts of its subtending cotyledons, was cut from the dorsal side of a dry seed using a Proxxon circular saw (blade thickness 0.1 mm, diameter 22 mm) rotating at a speed of 20 000 rpm (Prox-Tech Inc., Hickory, NC, USA). The specimen was hydrated with tap water until the coat could be separated from the cotyledons. Some seed coats isolated in this fashion were inspected with SEM and fluorescence microscopy according to Ma *et al.* (2004).

Measurement of hydrostatic hydraulic conductivity (Lp_h): A pressure probe similar to those used to measure water flow into and out of roots was modified for use with seed coats (Fig. 1A). Using a relatively large rod (4 mm diameter instead of the usual 1.5 mm), pressure changes could be induced for calculating the hydraulic conductivity (i.e. water flow in m^3 of water per m^2 surface area per second and per MPa of applied pressure difference). The glass capillary of the probe was 635 μm in diameter and 115 mm long. The cylindrical 'water reservoir' connecting the capillary with the seed coat had an 8 mm diameter and 9 mm depth (volume of ~450 mm^3; Fig. 1B). This provided a sufficient amount of water to be pushed across the coat in the presence of a pressure gradient (from 0.02 to 0.07 MPa) set up between the probe and the external medium. Pressures (P) in the probe were continuously recorded by a pressure transducer (26PC6FA6D; Pressure range: 0–172 MPa; Honeywell, Plymouth, Minnesota, USA) connected to a computer running the Pfloek software program (version 1.08; University of Bayreuth, Germany). Pfloek records pressure differences over time (rate constants and half-times) and measures the elasticity of the set-up (see below) required to evaluate water flows from $P(t)$ curves (Steudle and Heydt, 1988; Steudle, 1993).

Prior to mounting the seed coat, the probe and capillary were filled with silicone oil and the reservoir with water. Then, a circular piece of seed coat, isolated as described above, was draped over a rubber O-ring (7 mm outer diameter, 4 mm inner diameter) and inserted upside down on top of another rubber O-ring of the same size into the filled water reservoir (Fig. 1B). The seed coat was tightened into the reservoir in between the two rubber O-rings by a metal cylinder 'spacer' (7 mm outer diameter, 4 mm inner diameter) and a metal screw cap. As the screw cap was tightened, the cylinder squeezed the O-rings together, creating a watertight seal around the seed coat. According to the inner diameter of the coat disc, the surface area of the seed coat available for water flow was ~12 mm^2 (~$\pi \cdot 2^2$).

Once the coats were mounted, the pressure was allowed to stabilize at a value around 0 MPa, and then pressure relaxation experiments commenced. Each seed coat was tested with two independent pressure relaxations to get a mean half-time of water flow equilibration. A pressure relaxation involved quickly increasing the pressure by pushing a specific volume of water toward the seed coat. By monitoring the oil–water meniscus, the change in volume was kept constant. The Pfloek program recorded the initial pressure spike and its subsequent decrease with time, corresponding

to the movement of water across the seed coat. Once the pressure drop became linear, the initial slope of the line (k_w^{in}) was determined and used, along with the elastic modulus of the equipment, β (MPa×m^{-3}), and the seed coat surface area, A (m^2), to calculate Lp_h (m×s^{-1}×MPa^{-1}) according to:

$$Lp_h = \frac{k_w^{in}}{\beta \times A}. \quad (4)$$

For each seed coat, an average Lp_h was evaluated from the mean of two initial slopes. Between relaxations, measurements of β were conducted. This involved rapidly moving the meniscus toward the coat and measuring the change in volume (ΔV) produced, which referred to the corresponding change in pressure (ΔP) as described by Steudle (1993):

$$\beta = \frac{\Delta P}{\Delta V}. \quad (5)$$

For each seed coat, at least three pressure peaks were produced and the average β value calculated. Each cultivar was tested with ten replicate coats. Collected data were first transformed with the natural logarithm and then analysed in an unpaired *t*-test, assuming unequal variances, at a confidence level of $\alpha = 0.05$ with SAS (SAS Institute Inc., Cary, NC, USA).

Measurement of osmotic hydraulic conductivity (Lp_o) *and solute permeability* (P_s): A previously used osmometer (Steudle and Heydt, 1988) was modified for seed coat samples (Fig. 2). The lower reservoir of the osmometer was flooded with a solution of potassium ferrocyanide {$K_4[Fe(CN)_6]$} with an osmolality of ~45 mOsmol (~0.11 MPa of osmotic pressure) as measured cryoscopically with an osmometer (Osmomat 030; Gonotec, Berlin, Germany). A seed coat, outer side up, was draped over a rubber O-ring that had previously been placed around the lower reservoir. (In some experiments, living aleurone cells in the seed coat were killed by boiling the isolated coat in water for 5 min.) A teflon-coated grid (pore diameter of 185 μm) was placed on top of the coat to prevent its movement when internally pressurized. The grid was followed by a metal spacer, and finally a screw cap to tighten the assembly in place. The spacer and cap both had holes in the centre so that water and test solutes could be applied to the outer side of the seed coat.

Initially, distilled water was added to the upper reservoir, and the pressure building up in the osmometer was allowed to stabilize. Pressure was detected with a silicone pressure transducer (XTM-190M-7; maximum pressure: 0.34 MPa; Kulite Semiconductor Products Inc., Ridgefield, NJ, USA), and again recorded by the Pfloek program. The build-up of a pressure indicated that the seed coat had some selective properties allowing a fairly rapid passage of water but not of solutes, namely potassium ferrocyanide. Then the water was replaced by one of three treatment solutions of measured osmolality, i.e. $K_4[Fe(CN)_6]$, ethanol, or NaCl, and again the pressure was allowed to stabilize. After stabilization, the treatment solution was always replaced with distilled water so that an equilibrium pressure could be re-attained before adding the next test solution. The osmotic hydraulic conductivity of the seed coats (Lp_o) was measured from osmotic relaxation curves obtained following the addition of the non-permeating solute $K_4[Fe(CN)_6]$ to the upper chamber according to a procedure described earlier for

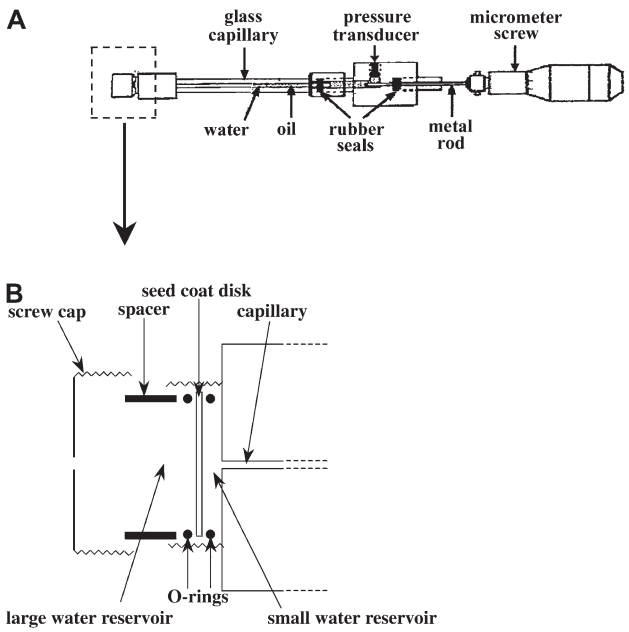

Fig. 1. Diagrams of the instrument used to measure the hydrostatic hydraulic conductivity of seed coats. (A) Pressure probe. (B) Enlarged and exploded sectional diagram of part of the pressure probe into which seed coat preparations were sealed (box in A). See Materials and methods for functional details.

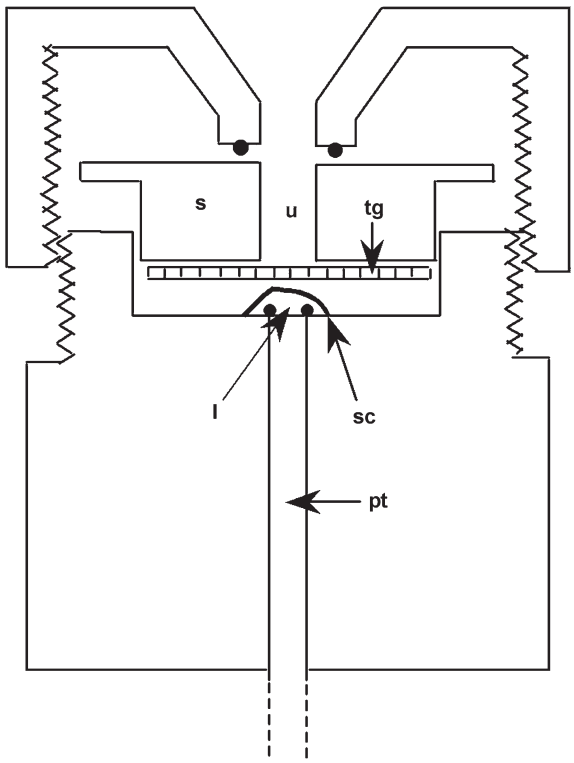

Fig. 2. Diagram of the instrument used to measure the osmotic hydraulic conductivities and solute permeabilities of seed coats. A dilute solution of potassium ferrocyanide {$K_4[Fe(CN)_6]$} was introduced into the lower compartment (l). Then the seed coat (sc) was draped over an O-ring. A teflon grid (tg) and spacer (s) were lowered onto the seed coat and the assembly tightened by screwing the upper part to the lower part. Liquid forced into the upper chamber (u) was removed and replaced with distilled water. The pressure in the lower chamber was measured by a pressure transducer (pt). After an equilibrium pressure had been reached, a test solute was added to the upper chamber.

artificial RO membranes (Steudle and Heydt, 1988). The equation used to measure Lp_o was:

$$Lp_o = \frac{V}{A} \times \frac{\ln(2)}{T^w_{1/2} \times (\varepsilon + \pi^i)} \quad (6)$$

where $T^w_{1/2}$ is the half-time of the pressure change that corresponded to water flow; $\varepsilon = \pi^i/[\pi^\circ/\Delta P] - 1$ (MPa), where π^i and π° refer to the osmotic pressures of the inner and outer chamber, respectively (MPa); V is the volume of the lower chamber (in m^3); and A is the surface area (m^2) of the seed coat preparation separating the two compartments. The permeability of the seed coats to NaCl and ethanol (P_s in $m \times s^{-1}$) was calculated from the resulting biphasic pressure relaxations typical of responses in the presence of permeating solutes (Steudle and Heydt, 1988). Solute permeability was estimated using a relationship analogous to that for the water:

$$P_s = \frac{V}{A} \times \frac{\ln(2)}{T^s_{1/2}} \quad (7)$$

where $T^s_{1/2}$ is the half-time of the pressure change that corresponded to the flow of the solute, *s*.

In the osmometer experiments, each treatment solution was tested twice per seed coat. Five seed coat replicates were used for each cultivar treatment. Lp_o and P_s data were transformed with the natural logarithm and then independently analysed in an unpaired *t*-test, assuming equal variances, at a 95% confidence interval with SAS (SAS Institute Inc.).

Results

Dimensions of seeds and anatomy

Soybean seeds were ellipsoid. Those from cv. Harovinton were larger (8.0–8.4 mm long by 6.8–7.2 mm wide by 5.4–6.0 mm high) than those from OX 951 (7.0–7.5 mm long by 5.0–5.5 mm wide by 4.8–5.1 mm high), measured with the hilum side down. Externally, four sides of a seed were distinguished, i.e. the ventral (containing the hilum, Fig. 3A), the dorsal (opposite to the ventral, Fig. 3B), and two intervening abaxial sides (Fig. 3C). Seed coats were typical for legumes (Corner, 1951; Esau, 1977) and consisted of four distinct layers (palisade, osteosclereid, crushed parenchyma, and aleurone, and sometimes associated crushed endosperm) and two cuticles (Fig. 3D, E). The sizes of the intercellular air spaces in the osteosclereid layer varied greatly, being largest near the hilum (100±14 μm high by 23±7 μm wide, Fig. 3F), grading to smaller at the abaxial side (36±7 μm high by 17±4 μm wide, Fig. 3G) and smallest on the dorsal part of the coat (8±3 μm high by 13±3 μm wide, Fig. 3H). The values given here were each the average ±SD of 24 spaces (three spaces per seed and eight seeds total).

Pattern of water uptake by soybean seeds

As seeds of cv. Harovinton took up water, they progressed through a sequence of externally visible changes. Imbibition of a typical seed, as seen from one of its abaxial sides, is illustrated in Fig. 4. Although some dry seeds had very small ridges on their dorsal sides (Fig. 3B), most were smooth coated (Fig. 4A). Within 45 min of being immersed in water, the coat on the dorsal side began to wrinkle (Fig. 4B). As imbibition continued, the affected area became larger (Fig. 4C, D). By 2 h, conspicuous ridges could also be seen on the abaxial sides near the hilum (Fig. 4E). Ridges became more numerous and extensive over the next hour (Fig. 4F–I), ultimately involving the whole seed except for the hilum. After this time, however, the seed coat became smoother as it ceased to enlarge while the embryo with its cotyledons continued to swell, filling more space within the coat (Fig. 4J–P). After ~9 h, the seed coat became smooth again as the embryo reached its maximum size (Fig. 4Q, R). This description is for a typical permeable seed, but there were variations in the timing of imbibition, and how the coat changed during hydration (data not shown).

The hydration pattern of the interior of the seed, consisting mainly of the two large cotyledons, was followed by dissecting off parts of the seed coat after various soaking times and observing the darker, hydrated tissue. Water entry into the cotyledons always began on the dorsal side under the wrinkled seed coat (Fig. 5A, B). Shortly thereafter, water penetrated into the cotyledons from the hilum and perhaps the abaxial sides. These initial cotyledonary wetting patterns always correlated with the locations of wrinkles in the overlying seed coat, with the exception of the hilum which only bulged outward. About 2–3 h later, the arched hydrated areas of the cotyledons approached each other (Fig. 5C). The cotyledons at the dorsal and hilum ends continued to hydrate, creating a slightly asymmetric, oval-shaped hydration front (Fig. 5D). The thickness of the hydrated tissue on all sides became more uniform with time as the front progressed toward the centre of the seed (Fig. 5E). Water absorption by the cotyledons continued until they were completely hydrated (after ~13–14 h of imbibition; Fig. 5F).

When the seed coats were removed prior to soaking, the hydration pattern of cotyledons was altered; they hydrated evenly over all their external surfaces from the outset. When the cotyledons did not separate, their hydration was uniform as described for the later stages in whole, intact seeds as in Fig. 5E. In most cases, however, the cotyledons did separate, allowing water to enter the space between them. Then, in addition to the hydration of the external surfaces, the internal surface (adaxial side) of each cotyledon started to hydrate, creating a semicircular wetting front (Fig. 5G). Due to this unusual and rapid wetting, the adaxial surfaces had a unique, wrinkled and flaky appearance (Fig. 5H) that presaged break up of the tissue as the cotyledons neared full hydration (Fig. 5I).

To test the importance of lateral water flow through the seed coat during imbibition, water was provided only to specific locations on the seed surface. In seeds hydrated only from the hilum side, water entered the seed coat and

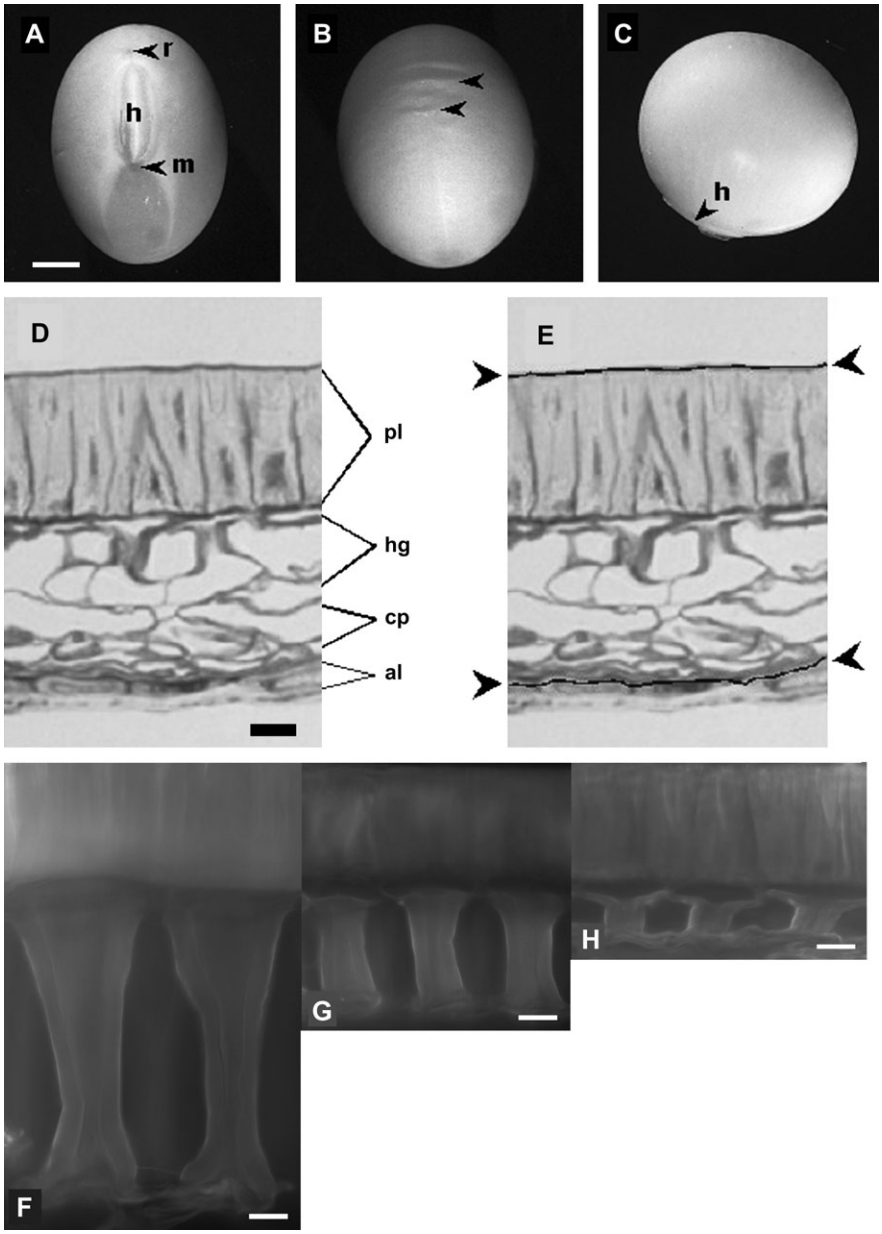

Fig. 3. Whole soybean seed and accompanying seed coat cross-sections (cv. Harovinton). (A–C) External views of a seed. (A) The ventral side. Note hilum (h), micropyle (m), and raphe (r). (B) The dorsal side with ridges (arrowheads). (C) One of the two abaxial sides with a side view of the hilum (h). Bar=2 mm. (D,E) Cross-section of a seed coat on the dorsal side. (D) Photomicrograph. The coat consisted of layers made up of the following cells: palisade (pl), osteosclereid or hourglass (hg), crushed parenchyma (cp), and aleurone (al). (E) Photomicrograph with the positions of the outer and inner cuticles indicated by solid lines between arrowheads. Photomicrograph courtesy of F Ma. Bar=15 μm. (F–H) Cross-sections of a coat taken from different sides of the seed. Notice the large changes in the heights of the osteosclereid (hourglass) cells and in the size of the intercellular spaces between them. (F) Near the hilum. (G) Central abaxial side. (H) Dorsal side. Bars=15 μm.

progressed upward along the abaxial sides, as evidenced by the wrinkling of the coat (Fig. 6A). The first areas of the cotyledons to be hydrated were adjacent to the hilum. However, water also moved circumferentially through the seed coat and from there into the adjacent regions of the cotyledons. Hence, an asymmetrical, oval-shaped hydration front was formed (Fig. 6B). In seeds hydrated from the dorsal side, initial water uptake was rapid and the areas of the cotyledons adjacent to the wrinkled coats were the first to hydrate (Fig. 6C). Lateral movement of the water was much less extensive than in the previous case, so that the hydration front had only a shallow concave shape as it moved dorsiventrally toward the hilum side (Fig. 6D). Of the seeds hydrated on one of their abaxial sides, only 13% took up water and, in these, a few wrinkles formed in the seed coat (Fig. 6E). Rates of imbibition were much slower than the hilum and dorsal hydrations. The cotyledon adjacent to the wrinkled seed

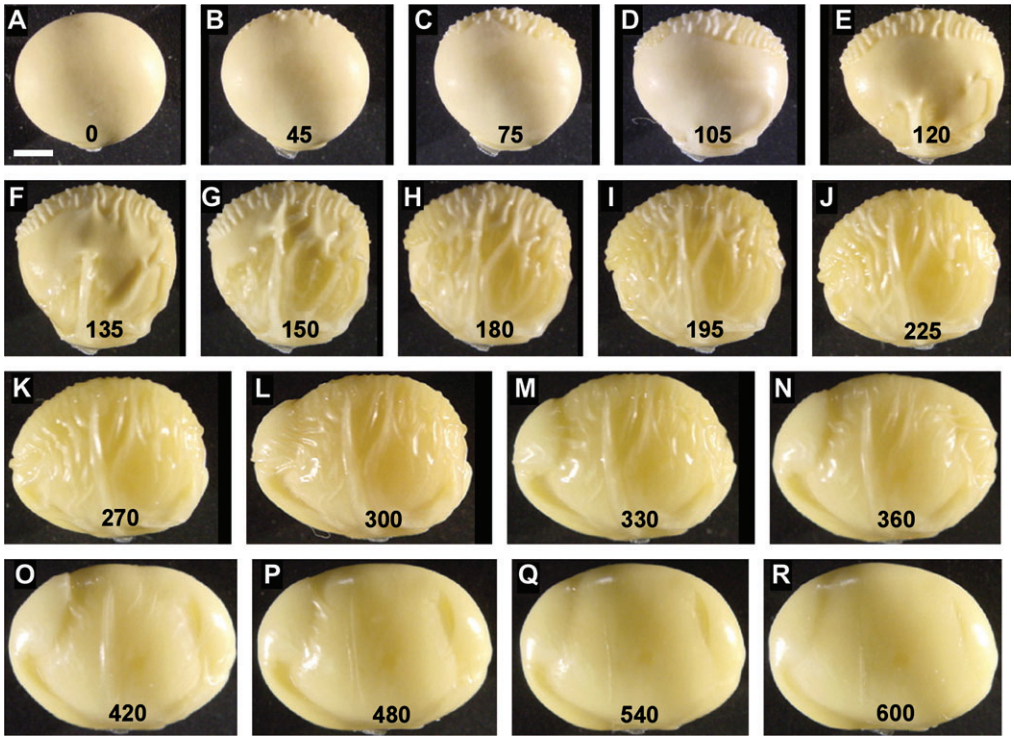

Fig. 4. Time series (A–R) hydration of a typical, individual soybean seed (cv. Harovinton). Numbers indicate the times (min) after the beginning of imbibition. Pictures illustrate external changes as a dry seed (0 min) becomes almost fully imbibed at 600 min (10 h). Bar=2 mm.

coat formed a slightly concave hydration front (Fig. 6F). When the localized hydration treatments were repeated with decoated seeds, the fronts were typically convex in all cases (Fig. 6G–I); this was most striking on the abaxial side (Fig. 6I). Differences between hydration by submersion and hydration of localized areas from wet filter paper were not due to variations in water supply, as normal hydration patterns were obtained from seeds entirely surrounded by wet filter paper.

Kinetics of water uptake by permeable and stone seeds with and without seed coats

Water uptake into intact, permeable seeds of cv. Harovinton commenced within 10 min, entered a more linear phase between 240 min and 540 min, and began to plateau after ~840 min (Fig. 7A). In striking contrast, stone seeds from cv. OX 951 took up no measurable quantities of water for the whole of this time (Fig. 7A). When seeds from which the coats had been removed were immersed in water, imbibition proceeded roughly twice as fast as that of intact Harovinton seeds. In this case, the initial phase of up to 45 min was rapid as the cotyledons hydrated (Fig. 7A). Water uptake by decoated stone seeds was just as quick as that by decoated permeable seeds (Fig. 7A).

When imbibition curves of intact seeds of cv. Harovinton were fitted exponentially according to Eq. (2), there was a good correlation (R^2=0.99, Fig. 7B). However, it was obvious that imbibition was more complex than indicated by Eq. (2). Initially, the rate of water uptake was relatively slow, suggesting a relatively low rate of imbibition of the outer part of the seed, i.e. of the coat. As the coat hydrated, its *Lp* increased, resulting in a second phase of hydration of the cotyledons with a higher initial rate. When the data of the initial phase were not incorporated in the exponential plot, the second phase appeared to be quite homogenous, i.e. Eq. (2) did apply (Fig. 7C).

During the imbibition of seeds of both varieties lacking a coat, the overall process could also be fitted exponentially with high correlation coefficients (Fig. 7D, F). However, here too there was an initial phase that differed from the rest. However, unlike the rate for intact seeds, initial phases were rapid, indicating a kind of diffusion-type kinetics for the swelling of the seed [see Eq. (3)] when terms with n >1 are neglected; see Materials and methods, and Discussion. Again, when the data points of the first phases were removed and the rest replotted, there was a homogenous slower phase of water uptake, as one would expect from diffusion kinetics (Fig. 7E, G).

Hydrostatic Lp

Measurements of hydrostatic hydraulic conductivity (Lp_h) were made of the hydrated, isolated coats from cvs Harovinton and OX 951. The surfaces of these showed no mechanical damage (as seen with fluorescence and SEM) caused by their hydration and removal from the cotyledons (data not shown). The four sharp spikes to the

Fig. 5. Hydration of cotyledons of permeable seeds (cv. Harovinton) obtained by totally immersing whole seeds (A–F) or decoated seeds (G–I). (A, B) A seed with dorsal wrinkles; coat partially dissected away. (A) Dorsal view. The hydrated cotyledon (*) corresponds to the wrinkled part of the seed coat (between arrows). (B) Abaxial view. The hydrated cotyledon (*) corresponds (arrows) to the wrinkled part of the seed coat. (C) Cross-section, hilum side down. Cotyledon hydration fronts from dorsal and hilum sides (arrowheads) have not yet merged. (D) Cross-section. Hydration fronts merged around cotyledons. The hydrated zone in cotyledons is thicker on the hilum side (between arrowheads) than on the dorsal side (between arrows). (E) Cross-section. Later stage of hydration in which the fronts have evened out and progressed further toward the centre of the seed. (F) Cross-section of a fully hydrated seed. (G) Seed that had been decoated prior to soaking. Water entered the cotyledons evenly on all surfaces, including those of the adaxial side (*). (H) Adaxial surface of part of a cotyledon. Note conspicuous flakes of tissue (arrows) and the uneven surface (arrowheads). (I) Adaxial side of a fully hydrated, decoated cotyledon. Note large cracks and extensive lifting of surface tissue (arrows). Bars=1 mm.

left in the graph in Fig. 8A were measures of changes in pressure resulting from specific changes in volume, so that the elastic modulus of the system (β) could be calculated as needed to calculate Lp_h [Eq. (4)]. The time-course of a pressure relaxation for a cv. Harovinton-derived coat began when a volume of water was displaced toward the coat to generate the driving force for water flow (Fig. 8A, right side of graph). Correction for momentum in the system quickly reduced this pressure to some extent, creating the initial sharp spike. Water continued to flow under pressure through the seed coat, gradually reducing the pressure in the chamber where it was being measured. The initial momentum spikes, with half-times of a fraction of a second, were not included in the Lp_h calculations. Instead, the longer second phase of the relaxation curves, representing water flow across the coat, was analysed.

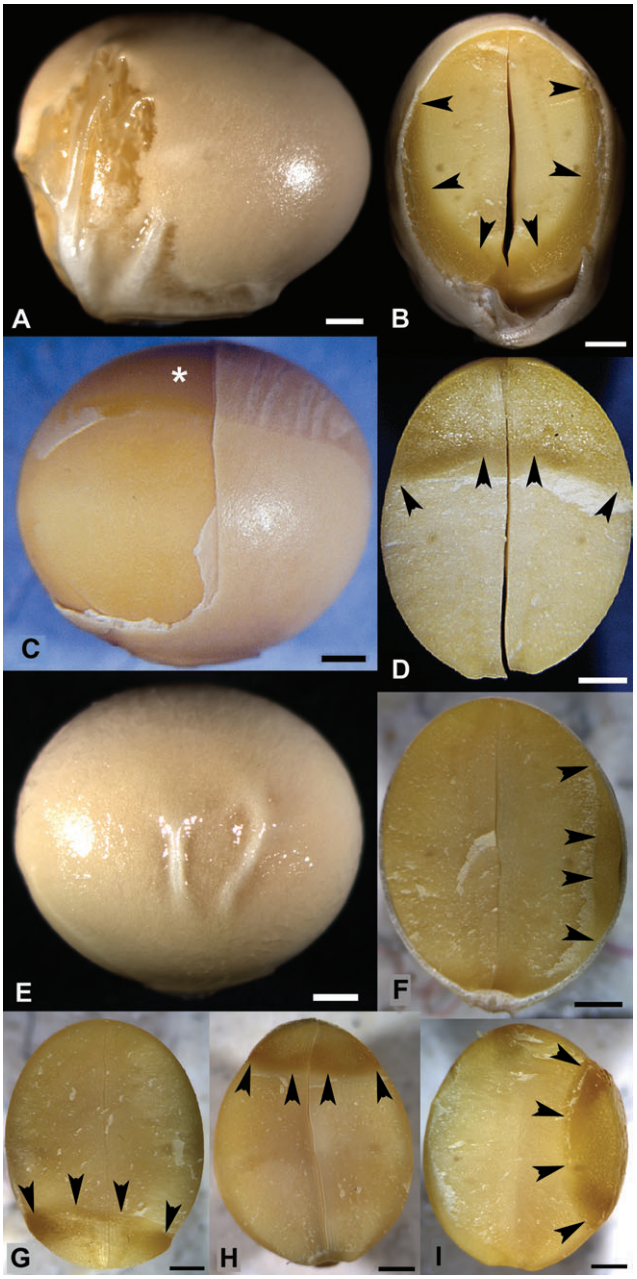

Fig. 6. Hydration of permeable seeds (cv. Harovinton) following localized application of water. (A, B) Seed hydrated through the hilum side. (A) External view of the seed. Wrinkles in the coat extend along one side (to the left in the photograph). (B) Cross-section through the seed. Cotyledon hydration was most advanced at the hilum end, and a cup-shaped hydrated zone extended along the abaxial sides of the seed; this zone would eventually reach the dorsal end. Concave hydration front indicated by arrowheads. (C, D) Seed hydrated through the dorsal side. (C) Whole seed with partially dissected coat. The hydrated cotyledon (*) was located under the wrinkled part of the coat. (D) Cross-section of a seed showing the concave hydration front (arrowheads). (E, F) Seed hydrated through the abaxial side. (E) Whole seed with two large ridges in the coat. (F) Cross-section of seed. Slightly concave hydration front in a cotyledon (arrowheads). (G–I) Cross-sections of seeds that had been decoated prior to localized applications of water. Hydration fronts were convex in all cases (arrowheads). (G) Hilum side hydration. (H) Dorsal side hydration. (I) Abaxial side hydration. Bars=1 mm.

Relaxation curves with steep slopes were obtained with seed coats of cv. Harovinton, indicating a rapid passage of water (Fig. 8A). On the other hand, seed coats of OX 951 transmitted the water much more slowly and, thus, the resulting rate of pressure reduction was much lower than that observed in cv. Harovinton coats (Fig. 8B). As seen in Table 1, the average Lp_h of the permeable cultivar, Harovinton, was ~5-fold (500%) greater than that of the Lp_h for OX 951 seed coats. The Lp_h for Harovinton was significantly greater than that for OX 951 at α=0.05 (n=10 coats per cultivar, t=4.43, P=0.0007). This 5-fold difference in Lp_h was applied to the water imbibition data for intact Harovinton seeds (Fig. 7A). It was assumed that the resulting line, positioned just above the intact OX 951 data, would represent the approximate imbibition values for hydrated coats of OX 951.

Osmotic properties of the seed coat

Isolated coats from permeable, impermeable, and heat-killed impermeable seeds exhibited properties of weak osmometers. Responses were variable, however, and there were no clear differences amongst the coats. With $K_4[Fe(CN)_6]$ in the lower chamber and distilled water in the upper, the pressure stabilized at a positive value (Fig. 9). Then the distilled water in the upper chamber was replaced by a more concentrated $K_4[Fe(CN)_6]$ solution, setting up a gradient that drew water from the lower chamber, lowering its pressure (Fig. 9A). Another stable pressure was reached after ~40 min, and this did not change even after many hours. When the solution in the upper chamber was changed back to distilled water, the osmotic gradient reversed and water slowly entered the lower chamber, once again increasing the measured pressure (data not shown). Osmotic hydraulic conductivities were calculated using the half-times of the pressure drops or increases; however, no significant differences were observed between cultivars at α=0.05 (n=5 coats per cultivar, t=0.52, P=0.61; Table 1). Although pressure equilibria were reached, the intensity of the reactions (i.e. the pressure drop or increase) was far less than that of a perfect osmometer. Using NaCl instead of $K_4[Fe(CN)_6]$ in the upper chamber resulted in the same changes (Fig. 9B). However, when ethanol was added to the upper chamber, biphasic curves were frequently obtained (Fig. 9C). In this case, water initially left the lower chamber, reducing the measured pressure. However, as the ethanol diffused from the upper chamber through the seed coat into the lower chamber, the osmotic gradient between the chambers was reduced, and the measured pressure rose again. When the ethanol was replaced with distilled water, a second biphasic curve was generated. This time, water was drawn into the lower chamber by the ethanol that had diffused into it. Then, as the ethanol diffused through the seed coat into the upper chamber, the osmotic gradient

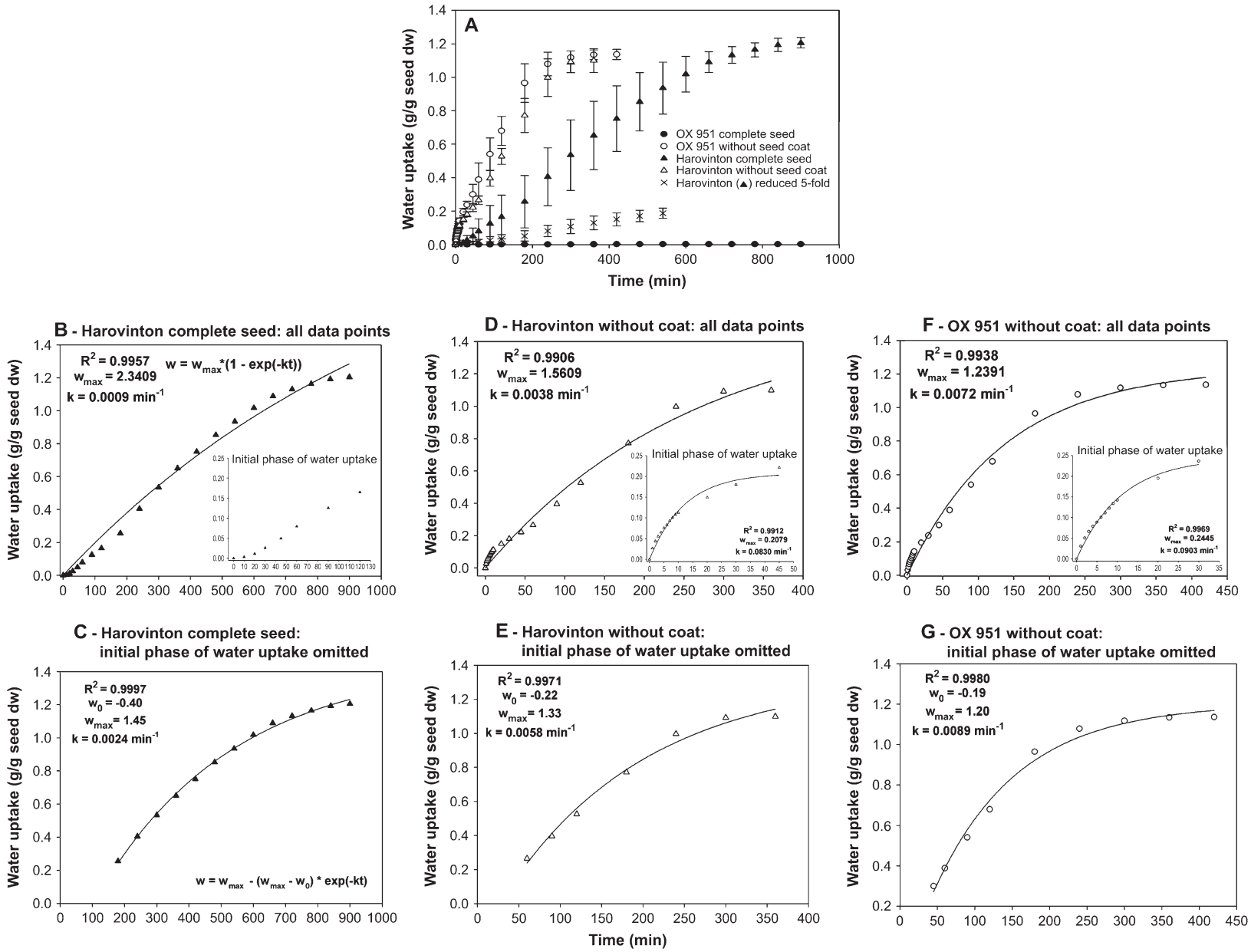

Fig. 7. Time-courses of soybean seed hydration, n=12 seeds. (A) Overview comparison of cvs OX 951 (stone seeds; circles) and Harovinton (permeable seeds; triangles) with and without seed coats. In addition, the linear part of the data from coated seeds of Harovinton (up to 540 min) was reduced by 5-fold and replotted (×). This represents the estimated water uptake of stone seeds if their coats could be hydrated, based on the 5-fold (500%) difference in hydraulic conductivity measured with the pressure probe (see Fig. 8). Bars indicate the SD. (B–G) Graphs and insets as titled, and fitted exponentially [Eq. (2)].

was again reduced and the pressure in the lower chamber decreased. Ethanol permeability was estimated from the second phase of the curves, but there were no differences between cultivars at α=0.05 (n=5 coats per cultivar, t=0.36, P=0.73; Table 1).

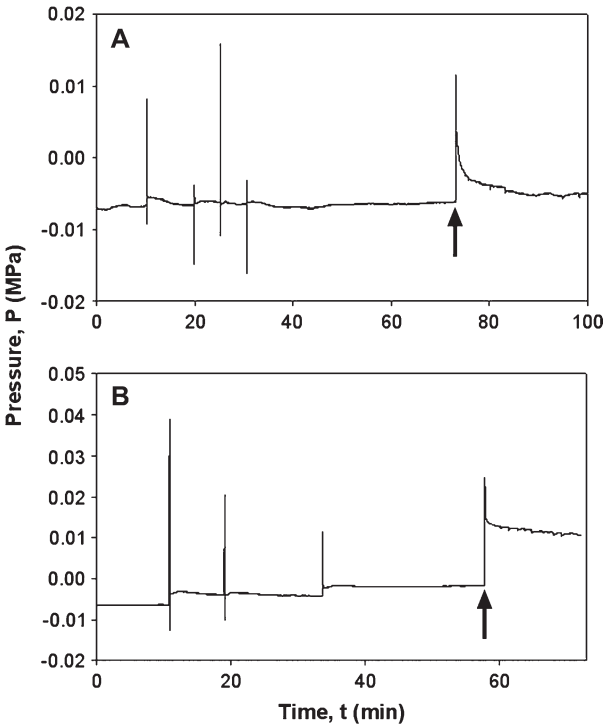

Fig. 8. Examples of hydrostatic *Lp* charts. Half-times are inversely proportional to Lp_h. Vertical lines on the left hand sides are pressure spikes used to calculate the tissue elastic modulus values (β). Pressure relaxations are indicated by arrows. (A) Seed coat of cv. Harovinton gave a short half-time. (B) Seed coat from stone seed of cv. OX 951 gave a long half-time.

Discussion

Hydration kinetics of permeable seeds

In agreement with the previous study of Ma *et al*. (2004), the earliest external sign of hydration of permeable seeds was a wrinkling of the dorsal seed coats. In seeds that already had small wrinkles, these were enlarged, and in seeds with smooth coats, similar wrinkles were created. These undulations formed when water was absorbed by the dry walls of the cells of the coat, increasing their volumes, and the force of this expansion was sufficient to separate the coat from the cotyledons in localized regions. The idea of Heil *et al*. (1992) that wrinkling ensues when water dissolves the middle lamella is not tenable, as pectic substances are not soluble in water at room temperature. Examples of solvents used for dissolving the middle lamella include 0.5% ammonium oxalate at 70–80 °C, a macerating solution including acetic acid, ethanol, and/or hydrochloric acid at 60 °C, or treatment in 5% pectinase at 37 °C (Jensen, 1962).

The initial stage of cotyledon hydration in intact soybean seeds could be predicted from external observations of the wrinkles in the seed coat. When seed coats were partially dissected away from the cotyledons, the position of the hydrated cotyledon parts in each seed correlated with the wrinkled dorsal area of the seed coat. Subsequently, water also passed through the hilum, wetting the cotyledons in this area; the hydrated hilum bulged outward during this process. When water was applied to specific sides of the seeds, the initial results were much the same in the dorsal and hilum sides. Movement of water into the abaxial sides was variable and usually absent (in 87% of the cases). When it did occur, abaxial hydration was slow and displayed a slightly concave front. Hahalis *et al*. (1996) and Chachalis and

Table 1. *Hydrostatic (Lp_h) and osmotic (Lp_o) hydraulic conductivity and solute permeability (P_s) values comparing hydrated seed coats of* Glycine max *with other plant tissues*

The values given are averages ±SD (n=10 for *Lp* and n=5 for P_s). Different letters in the first two columns indicate statistically significant differences (t-test, $P \leq 0.05$).

Specimen	Lp_h±SD×10^8 (m s^{-1} MPa^{-1})	Lp_o±SD×10^8 (m s^{-1} MPa^{-1})	P_s±SD×10^9 (m s^{-1})	Reference[a]
Glycine max				
cv. OX 951 seed coat	13±1 a	31±9 a, b	EtOH: 190±50 a NaCl: ND	1
cv. Harovinton seed coat	67±22 b	32±5 a, b	EtOH: 220±70 a NaCl: ND	1
Oryza sativa primary root	3.8–5.0	1.1–9.2	–	2, 3
Hordeum distichon primary root	0.3–4.3	0.3–4.3	–	4
Zea mays primary root	1–46	0.–5	Sucrose: 3.0 NaCl: 6–14	5–8
Allium cepa primary root	14	0.02–2	$NaNO_3$: 0.7	9, 10
Leaf cuticles	$\sim 1.7\times10^{-5}$–3.4×10^{-4}	–	–	11
Fruit cuticles	$\sim 4.3\times10^{-4}$–2.2×10^{-3}	–	–	11

[a] References: 1, this study; 2, Ranathunge *et al*. (2003); 3, Miyamoto *et al*. (2001); 4, Steudle and Jeschke (1983); 5, Steudle *et al*. (1987); 6, Steudle and Frensch (1989); 7, Zhu and Steudle (1991); 8, Peterson *et al*. (1993); 9, Melchior and Steudle (1993); 10, Melchior and Steudle (1995); 11, Riederer and Schreiber (2001).

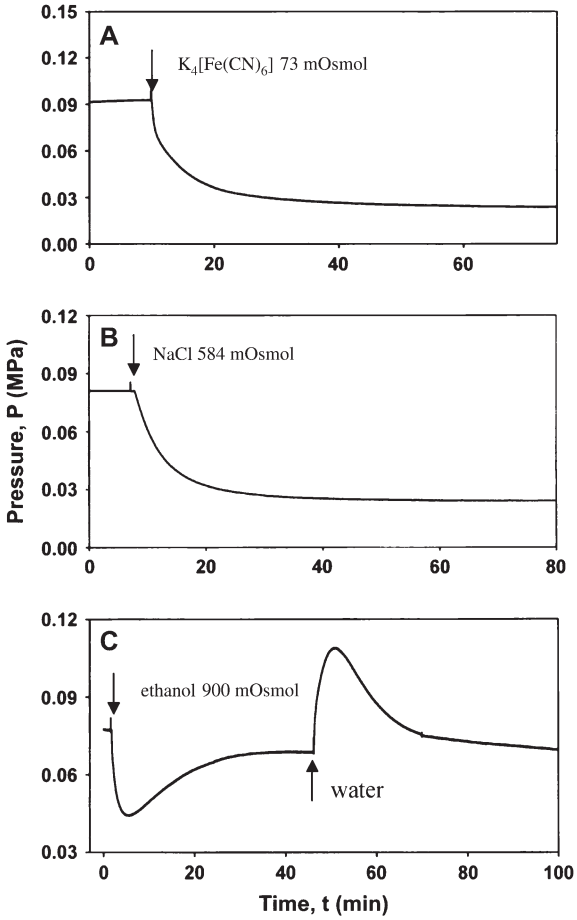

Fig. 9. Example charts of osmotic experiments from which seed coat permeabilities to various solutes were calculated. (A) Heat-killed seed coat from cv. OX 951. A solution of $K_4[Fe(CN)_6]$ with an osmotic pressure of 42 mOsmol (~0.1 MPa) was added to the lower chamber, and distilled water to the upper one. After a stable pressure was reached, the water in the latter was replaced by a 73 mOsmol solution of $K_4[Fe(CN)_6]$ as indicated by the arrow. (B) Seed coat from cv. Harovinton. The lower chamber contained a 45 mOsmol solution of $K_4[Fe(CN)_6]$. After pressure stabilization, NaCl (a 584 mOsmol solution) was added (arrow). (C) Heat-killed seed coat from cv. OX 951. The lower chamber contained 45 mOsmol $K_4[Fe(CN)_6]$. Ethanol (900 mOsmol) and distilled water were added to the upper chamber as indicated (arrows).

Smith (2000), who worked with soybean cvs KWS-E and Sapporo, reported that the rate of water uptake strictly at the hilum side was much less than that at the dorsal and abaxial sides. Their contrasting results could have been due to varietal differences, or to inadvertent wetting of the dorsal and hilum sides since water creep was apparently not prevented with a waterproof barrier.

As imbibition of whole seeds proceeded, hydration fronts became concave, indicating that either the edges of the cotyledons or the seed coat had preferentially transmitted water laterally. When the water supply was limited to the dorsal, hilum or abaxial sides, the front shapes were concave in coated seeds but convex in decoated seeds, proving that the circumferential movement had occurred through the coats. Such a role for the seed coat has been described earlier by McDonald *et al.* (1988). The lateral movement of water was more rapid on the hilum side, the location of the largest air spaces in the osteosclereid layer.

In trials with intact seeds, hydration did not commence from the adaxial (inner) surfaces of the cotyledons. These were appressed together tightly enough to prevent noticeable water entry to this area. On the other hand, when the seeds were decoated, the cotyledons usually separated enough to allow water to contact their adaxial surfaces, and water was absorbed evenly through these. However, Pietrzak *et al.* (2002), who used nuclear magnetic resonance imaging (NMR) to observe water entry into soybeans of cv. Colibri, interpreted their data in terms of a free movement of water in the 'void' between the cotyledons. Unfortunately, their observation intervals were too far apart (30 min) to allow observation of the initial imbibition patterns.

Role of the seed coat in hydration of permeable versus stone seeds

The dramatic difference between the lack of hydration of stone seeds (from cv. OX 951) and the rapid hydration of permeable seeds (from cv. Harovinton) is clearly a feature of the seed coat, as seen from the experiments where the coat was removed prior to soaking. During the most linear phase of the hydration, embryos without coats absorbed water more than twice as fast as those of coated Harovinton seeds, a result that is similar to the findings of others (Larson, 1968; Bewley and Black, 1978; Powell and Matthews, 1978; McDonald *et al.*, 1988; Chachalis and Smith, 2000). The rapid hydration of the isolated embryos caused them to break apart during the later stages of imbibition, an observation also in agreement with several previous reports and with the well-known role of the seed coat in modulating water delivery to the embryo (see Introduction). Unlike the abaxial faces of the cotyledons that remained quite smooth even during later stages of rapid hydration, the adaxial faces developed folds and produced large flakes of tissue. This face and the edges of the cotyledons were prone to cracking after longer hydration times.

Additional information on the role of the seed coat during the hydration of permeable seeds was gained from a detailed analysis of the imbibition curves. Water uptake by permeable seeds, both intact and decoated, exhibited two distinct phases: an initial one and a longer subsequent phase that was exponential (i.e. consistent with first-order kinetics). In the case of decoated seeds, the initial phase was rapid as the cotyledons began to hydrate evenly over their exposed surfaces. However, as this proceeded, the uptake of water slowed down and became exponential, probably due to the hydrated layers within the cotyledons becoming thicker and, therefore, less conductive so that the

hydration of the inner parts was increasingly delayed [see Eq. (2)]. The issue has been dealt with both theoretically and experimentally for plant tissue (Philip, 1958; Molz and Ikenberry, 1974; Steudle and Boyer, 1985; Westgate and Steudle, 1985; Steudle, 1992) in terms of diffusion kinetics ['diffusivity'; see Eq. (3)]. It has been also shown for seeds in key papers (Phillips, 1968; Waggoner and Parlange, 1976; Vertucci, 1989). Figure 10 demonstrates semilog plots of water uptake according to Eq. (2). For whole seeds of Harovinton (Fig. 10A), the initial phase was linear (constant k), but the rate was relatively slow due to coat hydration. Then the rate increased as seeds moistened. In decoated seeds (Fig. 10B), the initial phases of semilog plots were curvilinear (up to t=20 min), and uptake rates were fairly rapid. However, as rates slowed down, the overall uptake became exponential to a good approximation, as expected from typical diffusion kinetics [see Materials and methods and Eq. (3)]. The fact that there was a fairly long linear part may indicate that (i) diffusion kinetics could be used to describe uptake in the absence of coats and (ii) the changes in the diffusivity (D) were relatively small. In both cases (Fig. 10A, B), when the seeds approached saturation, it was difficult to measure the uptake rates accurately because of uncertainties in the true final weight (w_{max}). Therefore, the semilog curves would bend either upwards or downwards depending on the estimated w_{max}. On the other hand, the accuracy of the w_{max} measurements was better than ±SD of w, so the convex bending of the curves was instead due to increasing diffusivities as the seeds moistened.

When the water uptake of coated seeds was analysed, curves were homogenous and exponential provided that the initial slow phase was omitted, which we attribute to soaking of the coat with water. The intact seeds apparently have a rate limitation at the coat rather than in the interior of the seed. This means that measurements of the Lp_h or Lp_o of seed coats should be quite important for understanding the hydration pattern of seeds. However, this would require that coats be removed from the seeds without significant alterations that could artificially increase their hydraulic conductivity. Of course, the absolute values of coat Lp_h and Lp_o would relate to the rate constants (half-times) of the exponential part of swelling curves. However, calculations of Lp_h and Lp_o from uptake rates would only be possible if the forces driving water flow across the coats were known as well, i.e. the differences in water potential between the outside and inside of seeds.

Following seed imbibition in more detail is necessary to verify the idea of diffusion kinetics in quantitative terms. However, this would require a non-destructive method to measure the progression of internal hydration. In the case of intact seeds, the first phase was a lag mainly representing the need first to hydrate the seed coat, a process beginning from the dorsal side, followed by the hilum side, and eventually extending around the whole seed

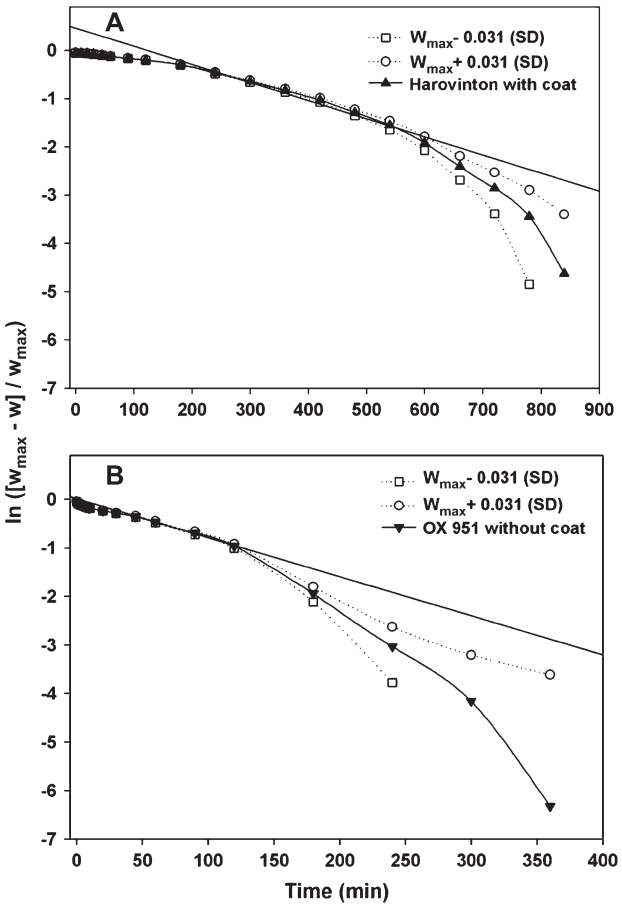

Fig. 10. Semilog plots of relative water uptake [Eq. (2)]. (A) For intact Harovinton seeds, the initial phase of imbibition was slow (small slope) due to the resistance of the coat. Once the coat was hydrated, the rate (slope) increased to linear (exponential phase). The linear part of the line indicated a constant diffusivity and was fitted between 180 min and 600 min. (B) For decoated OX 951 seeds, the initial uptake rate was fairly rapid and the overall rate became exponential as is typical of diffusion kinetics [Eq. (3)]. The linear part of this line was fitted between 30 min and 120 min. In both cases (A, B), when the seeds approached saturation, errors in measuring w_{max} increased. This is evident when w_{max} is artificially increased or decreased by the value of the standard deviation because the curves bend upward or downward, respectively. However, since the accuracy in measuring w_{max} was better than ±SD of w, it is concluded that the convex bending of the curves was not due to the uncertainty in measuring w_{max}. Rather, diffusivities (rates) increased as seeds became moistened. Filled triangles indicate data from Fig. 7A inputted into Eq. (2); open squares or circles indicate the same data as the filled triangles except the w_{max} was increased or decreased by its standard deviation.

coat. The remainder of the imbibition process was then nicely exponential, but slower than that for the decoated seeds. This suggested that the hydrated coat, now more permeable than it was initially, was still rate-limiting for water uptake rather than the progressive hydration of the embryo. It is indicated in the Results that, at least for soybean, some caution is necessary when interpreting overall seed imbibition in terms of first-order kinetics as has been done in the past [Leopold, 1983; Eq. (2)]. The fact that good correlations were obtained in the experiments of

other authors does not prove simple first-order kinetics as shown here. A closer look at water uptake is required.

Permeabilities of isolated seed coats to water and solutes

Using a pressure probe, it was possible to measure the permeability of isolated, hydrated seed coats to water directly. In view of the water-resistant properties of the dry stone seed coats, one might have expected that they would have a very low permeability to water even when hydrated. However, their Lp_h was, on average, smaller than that of the permeable seed coats by 'only' a factor of five or 500%. At first sight, the permeability of stone seed coats seems much higher than expected. However, one has to consider that during removal of coats from the embryos (although carefully done by imbibition after excising part of the seed), some alteration, namely to the outer side, may have occurred. Even when using completely intact coat preparations, the access of water to the inner side caused rapid hydration and expansion of the coat that may have increased its Lp_h. Hence, the relatively small difference between hydrated coats of cvs Harovinton and OX 951 of 'only' a factor of five is understandable. The high variability in the Lp_h values obtained for the seed preparations also indicates that some damage may have been done to the outer part of their coats. These ideas remain speculative as no cracks visible with SEM or fluorescence were introduced to the coats of hydrated OX 951 seeds. They do indicate that once the coats of stone seeds are hydrated, they are capable of conducting water, and one would expect to observe a slow imbibition if this were to occur in whole seeds. The fact that such an imbibition does not occur indicates that in whole seeds, the seed coat is not hydrated, and this is consistent with the finding that such seeds are covered with a continuous outer cuticle (Ma *et al*., 2004). Using a pressure probe for measuring the hydraulic conductivity of roots and cells is well established. Although there is confidence in the methods for isolating and fixing seed coats, some improvements may be possible.

When the current results were compared with previous measurements of water permeability of roots, or of cuticles from leaves and fruits, it was evident that hydrated seed coats were more permeable (Table 1). This is plausible because, in roots, the presence of an endodermis and often an exodermis, both containing Casparian bands and frequently suberin lamellae, can restrict radial water transport. For leaves and fruits that are constantly exposed to the atmosphere, their cuticles must be highly effective at retaining water to prevent desiccation. Although the water permeabilities of leaf and fruit cuticles are variable between tissues and species, they are typically much lower than those observed for soybean seed coats (see Tables 1 and 2 in Riederer and Schreiber, 2001). The much smaller hydraulic conductivity of cuticles as compared with seed coats should be due to the fact that, in the latter, a continuous cuticle is missing. Additionally, seed coats are more permeable to water because they are composed of dead cells and, thus, do not have cell membranes that are assumed to have a smaller hydraulic conductivity than the porous apoplast of living tissue (Steudle and Peterson, 1998).

Isolated seed coats were tested for their ability to act as osmometers. One would expect that most of the resistance to water and solute flow through the seed coat would be provided by its two, thin cuticles, one covering the palisade layer and the other the aleurone layer (Fig. 3E; Ma *et al*., 2004). If these are intact, typical cuticles, they should repel water and hydrophilic solutes and it could be assumed that the seed coats would not behave as osmotic barriers with a reasonable selectivity (high reflection coefficient). It was surprising, therefore, to find that this was not the case. The coats of both cvs Harovinton and OX 951 did show distinct, although weak, osmotic properties and some selectivity of solutes against water as revealed in the osmometer experiments. However, compared with cell membranes, these osmotic responses were small. The observed osmotic properties were not a function of the aleurone, the only layer of cells in the coat with some living cells (Yaklich *et al*., 1992; Ma *et al*., 2004), since killing the remainder of these cells did not alter the osmotic properties of the seed coats. In the presence of the osmolyte $K_4[Fe(CN)_6]$ (considered to be quite wall impermeant; Ranathunge *et al*., 2005), the pressures built up in the osmometer were substantially lower than one would expect for a reflection coefficient of unity. Osmotic responses to the 'impermeant' polar solute $K_4[Fe(CN)_6]$ just consisted of one 'water phase', indicating an indiscernible permeation of this solute. This was most probably due to repulsion of the $[Fe(CN)_6]^{4-}$ ion by fixed negative charges in the walls of the cells. Similarly, NaCl was also not measurably permeant. In contrast, the uncharged, small solute ethanol did permeate, creating biphasic responses in pressure like those of artificial membranes and also of living plant cells, but with much longer half-times (Steudle and Tyerman, 1983; Steudle and Heydt, 1988; Ye *et al*., 2004). In the case of coats from Harovinton, it was surprising that a pressure equilibrium could be reached, as the continuity of the outer cuticle is known to be interrupted by small cracks (Ma *et al*., 2004). Their reaction times to solution changes were slow compared with those of a living cell (Steudle and Tyerman, 1983; Ye *et al*., 2006) and the pressure changes obtained were far below those of a perfect osmometer (Table 1). These results indicate that the part of the seed coat providing the resistance to salt but not ethanol is a lipophilic structure and is, perhaps, the inner cuticle of the coat.

The fact that seed coats behave as weak osmotic barriers should be important in view of the fact the coats are said to retain solutes within the seed, at least to some extent

(Larson, 1968; Parrish and Leopold, 1977; Bewley and Black, 1978; Powell and Matthews, 1978; Duke *et al*., 1983). This means that the loss of valuable solutes (electrolytes, sugars, etc.) from embryos of swelling seeds would be limited. On the other hand, the rate of water uptake would be sufficient for embryo hydration due to a relatively high seed coat *Lp*. It is thought that these properties are caused by the composite structure of the coats which contain thin cuticles and layers of cell walls that would have differing hydraulic properties.

In conclusion, the present research has provided a variety of information related to the hydration of soybean seeds. Water initially enters the coat of a permeable seed from the dorsal side, and shortly after from the hilum side, wetting the adjacent parts of the cotyledons. Lateral water movement through the osteosclereid layer is minor at the dorsal end (where the intercellular spaces are smaller), but is extensive at the hilum end (with larger air spaces). When seed coats were present, they dominated the overall water uptake at any stage. Hence, except for a short period required for the hydration of coats, imbibition curves were exponential. Different from literature data, the present report provides detailed data from the beginning stages of imbibition, showing that there is a slow initial phase of water uptake that was interpreted in terms of seed coat hydration. The slow phase was followed by a second, more rapid one attributed to the hydration of the cotyledons. The second phase was strictly exponential, again indicating a rate limitation by the hydrated coat. Decoated seeds from both varieties showed a diffusion type of kinetics of water uptake as theoretically expected. When coats of stone seeds were removed from the seed by hydration, their permeability to water increased but remained ~5-fold less than that of similarly treated coats from permeable seeds. From a physiological point of view, it is plausible that the water permeability of hydrated seed coats is greater than that of roots, and much greater than that of cuticles of leaves and fruits. According to their anatomy, hydrated coats of both stone and permeable seeds exhibited properties of a weak osmometer with low selectivity.

Acknowledgements

This research was supported by grants from the Deutscher Akademischer Austauschdienst (German Academic Exchange Service; DAAD) and the Natural Sciences and Engineering Research Council of Canada to CAP. We thank Burkhard Stumpf and Drs Qing Ye and Kosala Ranathunge for their excellent technical assistance, and for helping to prepare Figs 1, 2, 8, and 9. Dr Fengshan Ma contributed Fig. 3D and E, and also insights during many discussions.

References

Arechavaleta-Medina F, Snyder HE. 1981. Water imbibition by normal and hard soybeans. *Journal of the American Oil Chemists' Society* **1981,** 976–979.

Baskin JM, Baskin CC, Li X. 2000. Taxonomy, anatomy and evolution of physical dormancy in seeds. *Plant Species Biology* **15,** 139–152.

Bewley JD, Black M. 1978. *Physiology and biochemistry of seeds in relation to germination*. Berlin: Springer-Verlag, Vol. 1.

Calero E, West SH, Hinson K. 1981. Water absorption of soybean seeds and associated causal factors. *Crop Science* **21,** 926–932.

Chachalis D, Smith ML. 2000. Imbibition behavior of soybean (*Glycine max* (L.) Merrill) accessions with different testa characteristics. *Seed Science and Technology* **28,** 321–331.

Corner EJH. 1951. The leguminous seed. *Phytomorphology* **1,** 117–150.

Crank J. 1975. *The mathematics of diffusion* 2nd edn of the original 1956 print. Oxford: Oxford University Press.

Duke SH, Kakefuda G, Harvey TM. 1983. Differential leakage of intracellular substances from imbibing seeds. *Plant Physiology* **72,** 919–924.

Esau K. 1977. *Anatomy of seed plants*, 2nd edn. New York: John Wiley & Sons.

Hahalis D, Cochrane MP, Smith ML. 1996. Water penetration sites in the testa of soybeans (*Glycine max* L. Merril) during seed imbibition. *Sci Legumes* **3,** 218–226.

Heil JR, McCarthy MJ, Ozilgen M. 1992. Magnetic resonance imaging and modelling of water uptake into dry beans. *Food Science and Technology* **25,** 280–285.

Hill HJ, West SH, Hinson K. 1986. Effect of water stress during seedfill on impermeable seed expression in soybean. *Crop Science* **26,** 807–812.

Jensen WA. 1962. *Botanical histochemistry: principles and practice*. San Francisco: WH Freeman and Co.

Kramer PJ, Boyer JS. 1995. *Water relations of plants and soils*. Orlando, FL: Academic Press.

Larson LA. 1968. The effect soaking pea seeds with or without seedcoats has on seedling growth. *Plant Physiology* **43,** 255–259.

Leopold AC. 1983. Volumetric components of seed imbibition. *Plant Physiology* **73,** 677–680.

Ma F, Cholewa E, Mohamed T, Peterson CA, Gijzen M. 2004. Cracks in the palisade cuticle of soybean seed coats correlate with their permeability to water. *Annals of Botany* **94,** 213–228.

McDonald MB, Vertucci CW, Roos EE. 1988. Seed coat regulation of soybean seed imbibition. *Crop Science* **28,** 987–992.

Melchior W, Steudle E. 1993. Water transport in onion (*Allium cepa* L.) roots. Changes in axial and radial hydraulic conductivities during root development. *Plant Physiology* **101,** 1305–1315.

Melchior W, Steudle E. 1995. Hydrostatic and osmotic hydraulic conductivities and reflection coefficients of onion (*Allium cepa* L.) roots. In: Baluska F, Ciamporova M, Gasparikova O, Barlow PW, eds. *Structure and function of roots*. Dordrecht, The Netherlands: Kluwer Academic Press, 209–213.

Miyamoto N, Steudle E, Hirasawa T, Lafitte R. 2001. Hydraulic conductivity of rice roots. *Journal of Experimental Botany* **52,** 1835–1846.

Molz FJ, Ikenberry E. 1974. Water transport through plant cells and cell walls—theoretical development. *Soil Science Society of America Journal* **38,** 699–704.

Parrish DJ, Leopold AC. 1977. Transient changes during soybean imbibition. *Plant Physiology* **59,** 1111–1115.

Peterson CA, Murrmann M, Steudle E. 1993. Location of major barriers to water and ion movement in young roots of *Zea mays* L. *Planta* **190,** 127–136.

Philip JR. 1958. Propagation of turgor and other properties through cell aggregations. *Plant Physiology* **33,** 271–274.

Phillips RE. 1968. Water diffusivity of germinating soybean, corn and cotton seed. *Agronomy Journal* **60,** 568–571.

Pietrzak LN, Fregeau-Reid J, Chatson B, Blackwell B. 2002. Observations on water distribution in soybean seed during hydration processes using nuclear magnetic resonance imaging. *Canadian Journal of Plant Science* **82,** 513–519.

Powell AA, Matthews S. 1978. The damaging effect of water on dry pea embryos during imbibition. *Journal of Experimental Botany* **29,** 1215–1229.

Ranathunge K, Steudle E, Lafitte R. 2003. Control of water uptake by rice (*Oryza sativa* L.): role of the outer part of the root. *Planta* **217,** 193–205.

Ranathunge K, Steudle E, Lafitte R. 2005. Blockage of apoplastic bypass-flow of water in rice roots by insoluble salt precipitates analogous to a Pfeffer cell. *Plant, Cell and Environment* **28,** 121–133.

Riederer M, Schreiber L. 2001. Protecting against water loss: analysis of the barrier properties of plant cuticles. *Journal of Experimental Botany* **52,** 2023–2032.

Steudle E. 1992. The biophysics of plant water: compartmentation, coupling with metabolic processes, and flow of water in plant roots. In: Somero GN, Osmond CB, Bolis CL, eds. *Water and life: comparative analysis of water relationships at the organismic, cellular, and molecular levels*. Heidelberg: Springer-Verlag, 173–204.

Steudle E. 1993. Pressure probe techniques: basic principles and application to studies of water and solute relations at the cell, tissue, and organ level. In: Smith JAC, Griffith H, eds. *Water deficits: plant responses from cell to community*. Oxford: BIOS Scientific Publishers, 5–36.

Steudle E, Boyer JS. 1985. Hydraulic resistance to radial water flow in growing hypocotyls of soybean measured by a new pressure-perfusion technique. *Planta* **164,** 189–200.

Steudle E, Frensch J. 1989. Osmotic responses of maize roots. Water and solute relations. *Planta* **177,** 281–295.

Steudle E, Heydt H. 1988. An artificial osmotic cell: a model system for simulating osmotic processes and for studying phenomena of negative pressure in plants. *Plant, Cell and Environment* **11,** 629–637.

Steudle E, Jeschke WD. 1983. Water transport in barley roots. *Planta* **158,** 237–248.

Steudle E, Oren R, Schulze ED. 1987. Water transport in maize roots. *Plant Physiology* **84,** 1220–1232.

Steudle E, Peterson CA. 1998. How does water get through roots? *Journal of Experimental Botany* **49,** 775–788.

Steudle E, Tyerman SD. 1983. Determination of permeability coefficients, reflection coefficients and hydraulic conductivity of *Chara corallina* using the pressure probe: effects of solute concentrations. *Journal of Membrane Biology* **75,** 85–96.

Vertucci CW. 1989. The kinetics of seed imbibition: controlling factors and relevance to seedling vigor. In: Stanwood PC, McDonald MB, eds. *Seed moisture: CSSA special publication number 14*. Madison, WI: Crop Science Society of America, Inc, 919–924.

Waggoner PE, Parlange JY. 1976. Water uptake and water diffusivity of seeds. *Plant Physiology* **57,** 153–156.

Westgate ME, Steudle E. 1985. Water transport in the midrib tissue of maize leaves—direct measurement of the propagation of changes in cell turgor across a plant tissue. *Plant Physiology* **78,** 183–191.

Yaklich RW, Vigil EL, Erbe EF, Wergin WP. 1992. The fine structure of aleurone cells in the soybean seed coat. *Protoplasma* **167,** 108–119.

Ye Q, Kim Y, Steudle E. 2006. A re-examination of the minor role of unstirred layers during the measurement of transport coefficients of *Chara corallina* internodes with the cell pressure probe. *Plant, Cell and Environment* **29,** 964–980.

Ye Q, Wiera B, Steudle E. 2004. A cohesion/tension mechanism explains the gating of water channels (aquaporins) in *Chara*-internodes by high concentration. *Journal of Experimental Botany* **55,** 449–461.

Zhu GL, Steudle E. 1991. Water transport across maize roots. *Plant Physiology* **95,** 305–315.

Zimmermann HM, Steudle E. 1998. Apoplastic transport across young maize roots: effect of the exodermis. *Planta* **206,** 7–19.